Indian J. Applied & Pure Bio. Vol. 41(1), 621-634 (2026). **ISSN: 0970-2091**

Molecular Docking evaluation of *Hultholia mimosoides* (Lam.) E. Gagnon & G. P. Lewis phytoconstituents for Anticancer activity

J R Samartha, Sandeep Telkar, G C Sachin, G Megha, Pooja S. Rajaput, R Divakara and *H M Kumaraswamy

Department of Biotechnology, Kuvempu University, Jnanasahyadri, Shankaraghatta - 577451 (India)
Corresponding Author: drhmklab@gmail.com

Abstract

This study performed molecular docking and ADMET analysis on ten phytocompounds from Hultholia mimosoides to find potential mutant p53 modulators for Pancreatic Ductal Adenocarcinoma (PDAC). The crystal structure of the TP53-induced glycolysis and apoptosis regulator protein (PDB ID: 3DCY) was used as the target. Limonoate showed the strongest binding affinity to the target protein at -9.5 kcal/mol. Retronecine and 1-Hydroxytacrine were the most promising ligands, exhibiting high ligand efficiency, zero Lipinski violations, and excellent absorption profiles. The interactions suggest a mechanism for either restoring p53 function or mimicking its activity. The results support the therapeutic potential of these phytochemicals as novel plant-based therapies for pancreatic cancer.

Key words : Molecular docking. *Hultholia mimosoides,* Phytoconstituents, Anticancer activity, ADMET analysis.

Pancreatic ductal adenocarcinoma (PDAC) is a highly lethal malignancy, characterized by a five-year survival rate of less than 12% and a rapidly increasing global incidence[6]. In 2022 alone, over 510,922 new cases and 467,409 deaths were reported worldwide according to WCRF[9]. Epidemiological studies from India have revealed a threefold rise over the past three decades, and 95% of these cases were diagnosed at advanced stages, which highlights the urgent need for novel therapeutic strategies[1]. The dismal prognosis of PDAC is primarily due to its late diagnosis, aggressive metastasis, and resistance to conventional therapies like gemcitabine[3].

A central factor in PDAC pathogenesis is the mutation of the *TP53* gene, which encodes the tumour suppressor protein p53. Located on the short arm of chromosome 17, TP53 acts as a transcription factor that orchestrates cellular responses to various stressors, including DNA damage, aberrant proliferative signals, and oxidative. In its wild-type, p53 plays a pivotal role in maintaining genomic stability by inducing apoptosis in

response to cellular stress[4]. However, missense mutations, especially in the DNA-binding domain (*e.g.*, R273H), inactivate p53, enabling cancer cells to evade apoptosis. Mutant p53 is often associated with poor prognosis, metastasis, and chemoresistance, making it a prime therapeutic target[2].

Given these challenges, the search for natural compounds capable of restoring or mimicking p53 function has gained traction. Bioactive compounds rich in polyphenols and flavonoids are of particular interest due to their anti-inflammatory, antioxidant, and anticancer properties. Among them, *Hultholia mimosoides* (formerly *Caesalpinia mimosoides*), a leguminous climber native to tropical Asia, stands out. It is traditionally used as a food and remedy for fever and inflammation. *H. mimosoides* is rich in bioactive phytochemicals like gallic acid, cassane-type diterpenoids, homoisoflavonoids, and dibenzofuran.

Pharmacological studies have confirmed its antioxidant, anti-inflammatory, and cytotoxic properties. Notably, its leaf extract has been shown to reduce intracellular reactive oxygen species (ROS) and enhance stress resistance in *C. elegans*. These findings suggest the plant's potential as a safe, edible source of therapeutic agents.

This study investigates selected phytocompounds from *H. mimosoides* for their ability to interact with p53 through molecular docking, complemented by ADMET (Absorption, Distribution, Metabolism, Excretion, and Toxicity) profiling. Molecular docking enables prediction of the binding affinity and interaction mode between a ligand and the p53 protein, while ADMET profiling assesses the pharmacokinetic and safety characteristics essential for drug development.

Preliminary docking studies indicate that certain compounds bind effectively to critical residues in both WT and mutant p53, including Arg273, a mutation hotspot in PDAC. These interactions suggest a potential mechanism for restoring p53 function or mimicking its activity. Moreover, ADMET analysis reveals that several compounds exhibit favourable oral bioavailability, low toxicity, and metabolic stability.

In conclusion, this integrative in silico approach supports the therapeutic potential of *H. mimosoides*-derived phytochemicals as modulators of p53 in PDAC. These findings lay the groundwork for further in vitro and in vivo studies and may contribute to developing novel plant-based therapies targeting p53-related pathways in pancreatic cancer.

Protein preparation :

The crystal structure of the TP53-induced glycolysis and apoptosis regulator protein (PDB ID: 3DCY) from *Homo sapiens* (in .pdb format) was retrieved from the RCSB Protein Data Bank[7]. A clean structure file was prepared by removing water molecules, ions, and non-essential heteroatoms using PyMOL 3.0. Polar hydrogen atoms and Kollman charges were added, and the resulting receptor was converted to .pdbqt format for docking analysis using Auto Dock 1.5.7.

Ligand preparation :

Ten bioactive compounds from *Hultholia mimosoides* were selected and downloaded in 3D SDF formats from the PubChem

database. The 3D structures were subsequently energy-minimized and converted to .pdb format using Chem3D Pro. Polar hydrogen atoms and Gasteiger partial charges are added and converted to .pdbqt format for analysis using Auto Dock 1.5.7.

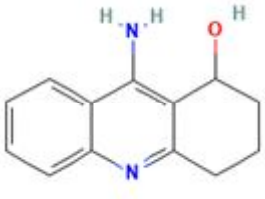

Figure 1. *1-Hydroxytacrine*

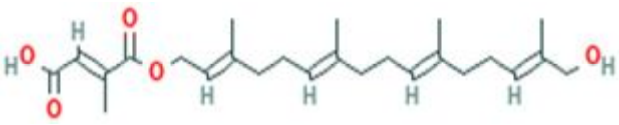

Figure 2. *Cavipetin D*

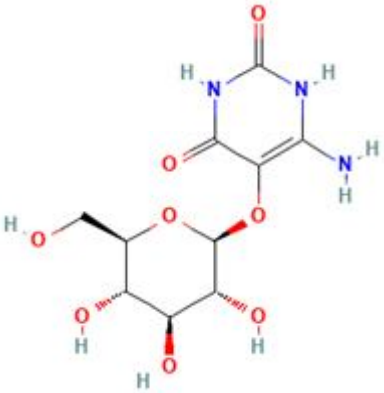

Figure 3: *Convicine*

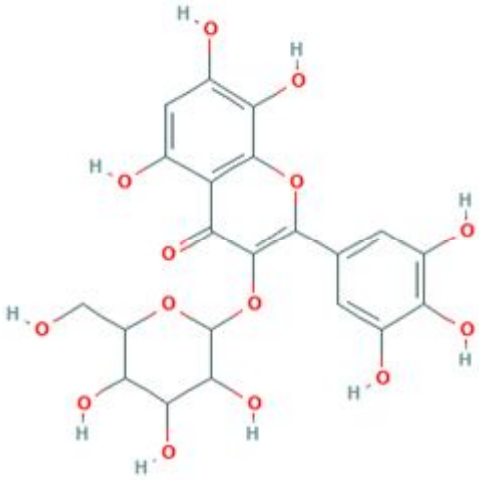

Figure 4: *Hibiscitrin*

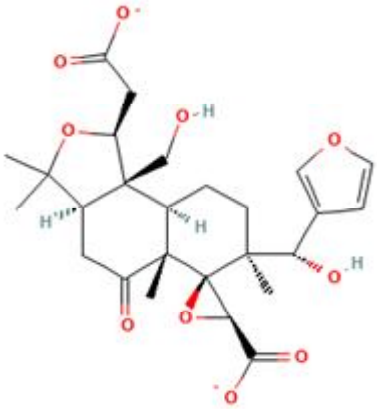

Figure 5: *Limonoate*

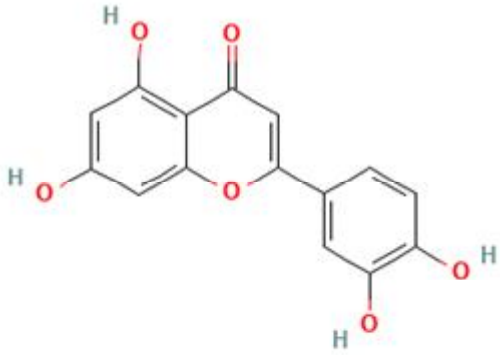

Figure 6: *Luteolin*

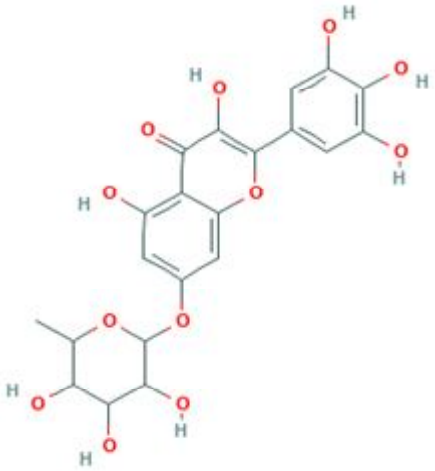

Figure 7: Myricetin 7-rhamnoside

Figure 8: Neoglucobrassicin

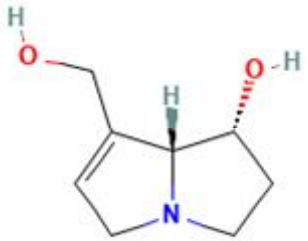

Figure 9: Retronecine

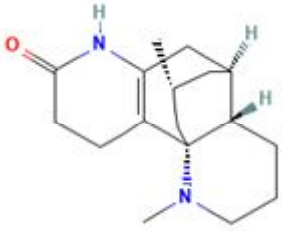

Figure 10: Sauroxine

Pharmacokinetic properties prediction :

The drug-likeness properties were determined by Lipinski's Rule of Five[5]. The molecular properties, Ligand efficiency (LE), lipophilic ligand efficiency (LLE), and ligand efficiency-associated lipophilic index (LELP) of the compounds were predicted using Data-Warrior V6.1.0 hosted at openmolecules.org[8].

The absorption, distribution, metabolism, and excretion (ADME) are the key parameters to assess the intense movement of drugs into the body. Early consideration of these pharmaco-kinetic features is essential for characterizing the integrity and potential efficacy of compounds in the drug design process. The pkCSM server was used to evaluate the ADME properties of the drug.

Toxicity prediction :

Toxicity prediction is an essential stage in modern drug design, measuring the degree of toxicity, which can have adverse effects on humans and animals. Therefore, the toxicity of the selected phytocompounds has been assessed through the pkCSM server. Various toxicological parameters were considered in this study.

Molecular docking :

The molecular docking study was performed to estimate the binding affinity of the identified bioactive compounds (ligands) toward the target protein, p53. The AutoDock Vina algorithm was used to identify the best docked conformation between the ligand and the protein. Active site prediction was performed using the PDBsum server. A receptor grid was generated in AutoDock 1.5.7, with a grid box size of X = 25.086, Y = 25.086, and Z = 25.086 for further analysis. All the docking runs were performed in Intel(R) Core (TM) i3-6006U CPU processor with 16 GB RAM. AutoDock Vina was compiled and run on Windows operating system. BIOVIA Discovery Studio 2021 Client, was used to infer the pictorial depiction of interaction between the ligands and the target protein.

Pharmacokinetic Properties Prediction :

Among the ten screened compounds, 1-Hydroxytacrine, Luteolin, Retronecine, and Sauroxine showed good drug-likeness with zero violations to Lipinski's rule, indicating favorable pharmacokinetic properties. Cavipetin D, Limonoate, and Neoglucobrassicin had one violation each, suggesting moderate drug-likeness. However, Convicine, Hibiscitrin, and Myricetin 7-rhamnoside violated two rules, mainly due to high hydrogen bond donors/ acceptors and molecular weight, indicating potential challenges in oral bioavailability. Overall, 1-Hydroxytacrine and Luteolin emerged as the most promising candidates (Table-1).

Retronecine and 1-Hydroxytacrine exhibited high ligand efficiency (LE: 0.6225 and 0.4662, respectively) with favorable LLE and LELP values, indicating strong binding with good drug-like properties. Convicine also showed good LLE (7.6413) despite moderate LE. In contrast, Cavipetin D and Limonoate had poor LE and highly unfavorable LELP values, suggesting inefficient binding and excessive lipophilicity. Overall, Retronecine and 1-Hydroxytacrine were the most efficient ligands (Table-2).

Table-1. Drug-likeness and molecular properties of selected screened Phytocompounds

Sl No	Compound	Pubc-hem ID	Hydrogen-bond donor	Hydro gen-bond acceptor	log p	Molecular weight (g/mol)	No. of Viola-tions
1	1-Hydroxytacrine	3655	2	3	1.7831	214.267	0
2	Cavipetin D	14527064	2	5	7.3735	418.572	1
3	Convicine	88000	7	11	-3.5858	305.242	2
4	Hibiscitrin	15559736	10	14	-1.0383	496.376	2
5	Limonoate	25201054	2	10	4.2726	504.53	1
6	Luteolin	5280445	4	6	1.99	286.238	0
7	Myricetin 7-rhamnoside	76594575	8	12	0.0819	464.378	2
8	Neoglucobrassicin	9576416	5	12	-0.4114	478.498	1
9	Retronecine	10198	2	3	-0.4289	155.196	0
10	Sauroxine	5462447	1	3	2.2265	274.406	0

Table-2. Ligand Efficiency and Lipophilic indices of Phytocompounds

Sl No	Compound	Ligand efficiency (LE)	Lipophilic ligande fficiency (LLE)	Ligand-corrected lipophilic efficiency (LELP)
1	1-Hydroxytacrine	0.46619	3.654	3.8248
2	Cavipetin D	0.084042	-5.5357	87.735
3	Convicine	0.26494	7.6413	-13.535
4	Hibiscitrin	0.070867	2.8463	-14.651
5	Limonoate	0.060918	5.8712	-70.136
6	Luteolin	0.14877	0.28733	13.376
7	Myricetin 7-rhamnoside	0.046386	1.0339	1.7656
8	Neoglucobrassicin	0.08934	2.4302	-4.6049
9	Retronecine	0.62252	5.4204	-0.68897
10	Sauroxine	0.1552	0.036113	14.346

Among the compounds, Retronecine, Sauroxine, and 1-Hydroxytacrine showed high intestinal absorption (>90%) and good Caco-2 permeability, indicating strong absorption potential. Luteolin also demonstrated excellent permeability but showed a negative intestinal absorption value, possibly due to a prediction anomaly. Cavipetin D had moderate absorption (90.67%) but poor permeability. Convicine, Hibiscitrin, and Neoglucobrassicin showed poor absorption (<20%) and low permeability, indicating limited bioavailability. Most compounds had moderate water solubility, except Luteolin, which was highly soluble. Only a few compounds acted as P-glycoprotein substrates, which may influence efflux and absorption profiles (Table-3a).

Retronecine, Sauroxine, and 1-Hydroxytacrine showed favorable distribution profiles with good volume of distribution (VDss), moderate unbound fractions, and the ability to cross the blood-brain barrier (log BB > 0.3). In contrast, Cavipetin D, Convicine, Hibiscitrin, and others showed poor BBB and CNS permeability. Myricetin 7-rhamnoside and Hibiscitrin had high VDss but limited brain access, suggesting peripheral distribution (Table-3b).

Most compounds were not substrates or inhibitors of key cytochrome P450 enzymes, indicating a low risk of metabolic interactions. Only Cavipetin D and Limonoate were CYP3A4 substrates, while 1-Hydroxytacrine and Luteolin inhibited CYP1A2, with Luteolin also inhibiting CYP2C9. Overall, metabolic liability appears low for most compounds, with minimal potential for enzyme-mediated drug interactions (Table-3c).

All compounds were non-substrates of renal OCT2, suggesting minimal renal transporter-mediated excretion. Cavipetin D showed the highest total clearance, indicating faster elimination, while other compounds like Retronecine, Convicine, and Limonoate showed moderate clearance rates. Overall, most compounds exhibited acceptable excretion profiles (Table-3d).

Table-3 a, b, ‘c and d: ADME Profile (Absorption, Distribution, Metabolism and Excretion) Phytocompounds

Table 3a :

Absorbtion	1-Hydro-xytacrine	Cavipe-tin D	Convi-cine	Hibis-citrin	Limo-noate	Lute-olin	Myric etin 7-rha-mnoside	Neoglu-cobras-sicin	Retro-necine	Sauro xine
Water solubility (log mol/L)	-3.104	-4.662	-2.389	-2.894	-2.683	0.096	-2.892	-2.739	-0.822	-3.163
Caco2 permeability (log Papp in 10^{-6} cm/s)	1.171	0.553	-0.557	-1.545	-0.291	81.13	-1.61	-0.693	1.435	1.539
Intestinal absorption (human) (% Absorbed)	94.029	90.671	18.305	17.423	41.967	-2.735	38.019	5.936	99.202	92.195
Skin Permeability (log Kp)	-2.761	-2.735	-2.735	-2.735	-2.735	Yes	-2.735	-2.735	-2.739	-3.247
P-glycoprotein substrate	Yes	No	No	Yes	Yes	No	Yes	Yes	No	No
P-glycoprotein I inhibitor	No	No	No	No	No	No	No	No	No	No
P-glycoprotein II inhibitor	No	Yes	No	No	No	No	No	No	No	No

Table 3b :

Metabolism	1-Hydro-xytacrine	Cavipe-tin D	Convi-cine	Hibis-citrin	Limo-noate	Lute-olin	Myricetin 7-Rhamnoside	Neogluco-brassicin	Retro-necine	Sauro xine
CYP2D6 SUBSTRATE	No	No	No	No	No	No	No	No	No	No
CYP3A4 SUBSTRATE	No	Yes	No	No	Yes	No	No	No	No	No
CYP1A2 INHIBITIOR	Yes	No	No	No	No	Yes	No	No	No	No
CYP2C19 INHIBITIOR	No	No	No	No	No	No	No	No	No	No
CYP2C9 INHIBITIOR	No	No	No	No	No	Yes	No	No	No	No
CYP2D6 INHTIOR	No	No	No	No	No	No	No	No	No	No
CYP3A4 INHIBITIOR	No	No	No	No	No	No	No	No	No	No

Table 3c :

Distribution	1-Hydro-xytacrine	Cavipe-tin D	Convi-cine	Hibis-citrin	Limo-noate	Lute-olin	Myric etin 7-rha-mnoside	Neoglu-cobras-sicin	Retro-necine	Sauro xine
VDss (human) (log L/kg)	0.549	-0.952	0.823	1.288	-0.159	1.153	1.575	-0.754	0.311	0.856
Fraction unbound (human)	0.33	0.054	0.802	0.282	0.584	0.168	0.167	0.471	0.507	0.556
BBB permeability (log BB)	0.43	-0.558	-1.142	-2.474	-1.025	-0.907	-1.966	-1.658	0.474	0.349
CNS permeability (log PS)	-1.99	-2.655	-3.989	-4.998	-3.338	-2.251	-4.319	-4.311	-2.974	-3.171

Table 3d :

Excretion	1-Hydro-xytacrine	Cavipe-tin D	Convi-cine	Hibis-citrin	Limo-noate	Lute-olin	Myric etin 7-rha-mnoside	Neoglu-cobras-sicin	Retro-necine	Sauro xine
Total Clearance (log ml/min/kg)	0.213	2.026	0.564	0.31	0.519	0.495	0.314	0.411	0.721	0.498
Renal OCT2 substrate	No	No	No	No	No	No	No	No	No	No

Toxicity Prediction :

Most compounds showed acceptable toxicity profiles with no skin sensitization. **Retronecine** had the highest chronic toxicity tolerance (LOAEL), while **Convicine**, **Hibiscitrin**, and **Myricetin 7-rhamnoside** also showed high chronic tolerance. **1-Hydroxytacrine**, **Convicine**, **Limonoate**, and **Neoglucobrassicin** were predicted to be hepatotoxic, which may limit their safety. Overall, **Luteolin**, **Sauroxine**, and **Cavipetin D** showed lower toxicity concerns.

Table-4. Toxicity Prediction Parameters for Selected Compounds this table Evaluates the safety profile including acute toxicity and hepatotoxicity

Excretion	1-Hydro-xytacrine	Cavipe-tin D	Convi-cine	Hibis-citrin	Limo-noate	Lute-olin	Myric etin 7-rha-mnoside	Neoglu-cobras-sicin	Retro-necine	Sauro xine
Max. tolerated dose (human) (log mg/kg/day)	0.119	-0.291	0.696	0.471	0.92	0.499	0.462	0.798	0.83	0.039
Oral Rat Acute Toxicity (LD50) (mol/kg)	2.588	1.901	2.528	2.515	2.397	2.455	2.553	2.631	2.482	2.559
Oral Rat Chronic Toxicity (LOAEL) (log mg/kg_bw/day)	1.333	0.403	3.346	3.914	1.642	2.409	3.389	3.905	5.559	0.683
Hepatotoxicity	Yes	No	Yes	No	Yes	No	No	Yes	No	No
Skin Sensitisation	No	No	No	No	No	No	No	No	No	No

Molecular docking :

Among the compounds, **Limonoate** showed the strongest binding affinity (-9.5 kcal/mol) through hydrophobic interactions without hydrogen bonds. **Hibiscitrin** and **Neoglucobrassicin** followed with a binding affinity of -9.0 kcal/mol, forming two and one hydrogen bonds, respectively, along with additional interactions like Pi-Cation and Van der Waals forces. **Convicine** also formed one hydrogen bond with a binding affinity of -8.8 kcal/mol. **Myricetin 7-rhamnoside** and **Luteolin** had slightly lower affinities (-8.7 and -8.1 kcal/mol) with limited hydrogen bonding, relying more on Pi interactions (Table-5).

Table-5. Molecular Docking Results and Binding Interactions with p53 Protein this table lists the binding affinities and specific amino acid interactions.

Sl. No.	Compound	Binding affinity	Amino acid involved in interaction	H-bond distance	Number of H-bond	Types of interactions
1	Limonoate	-9.5	TYR92, PRO115, ALA200	Nil	0	Alkyl, Pi-Alkyl
2	Hibiscitrin	-9.0	ARG203	3.06Å, 3.03Å	2	Hydrogen bond, Pi-Cation
3	Neoglucobrassicin	-9.0	THR230	3.00Å	1	Hydrogen bond, Van der waals, Pi-Cation, Amide Pi-Stacked
4	Convicine	-8.8	ARG10	3.03Å	1	Hydrogen bond, Alkyl
5	Myricetin 7-rhamnoside	-8.7	LEU100, ARG203	Nil	0	Pi-Cation, Pi-Alkyl
6	Luteolin	-8.1	ARG203	3.09Å, 3.17Å	2	Hydrogen bond, Pi-Cation

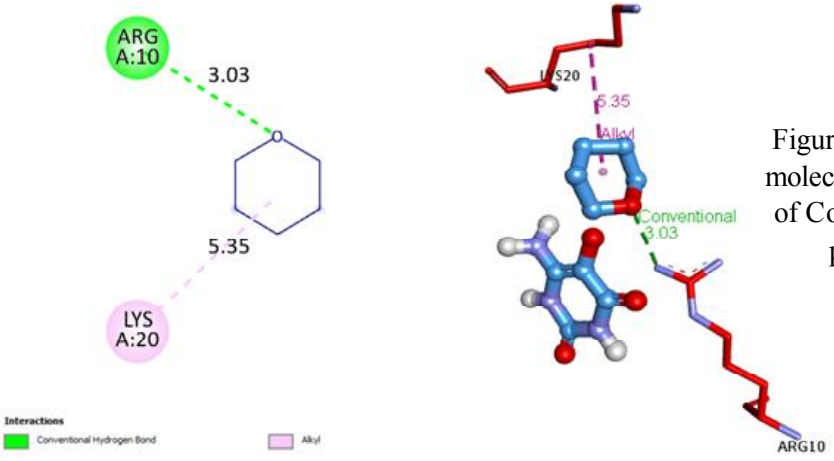

Figure 2. 2D and 3D molecular interactions of Convicine against p53 protein

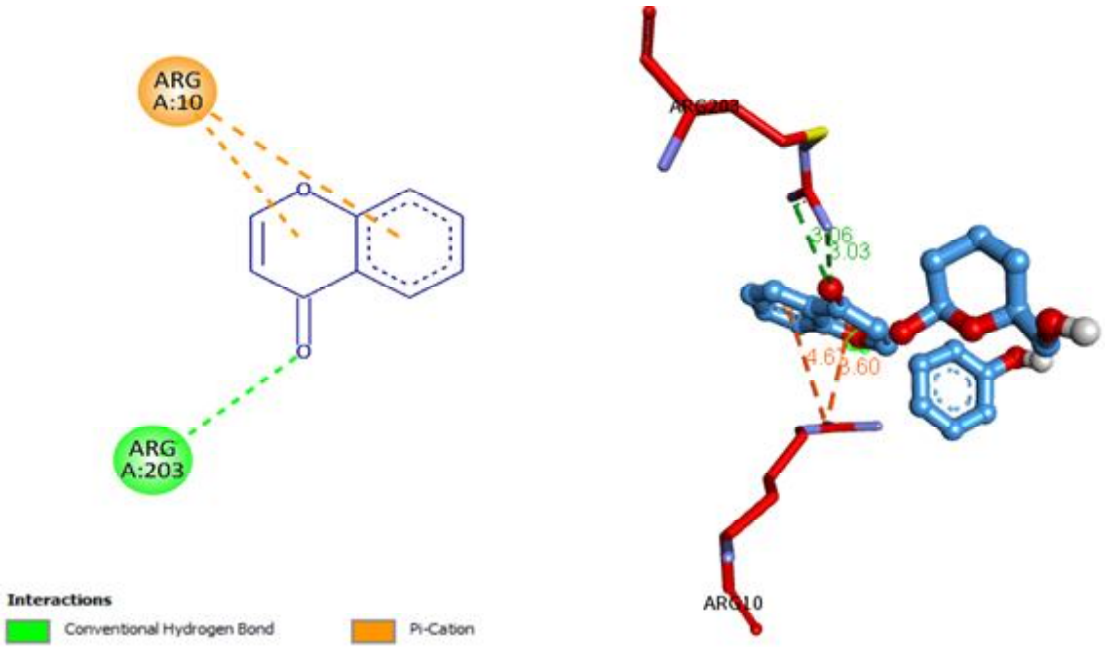

Figure 3. 2D and 3D molecular interactions of Hibiscitrin against p53 protein

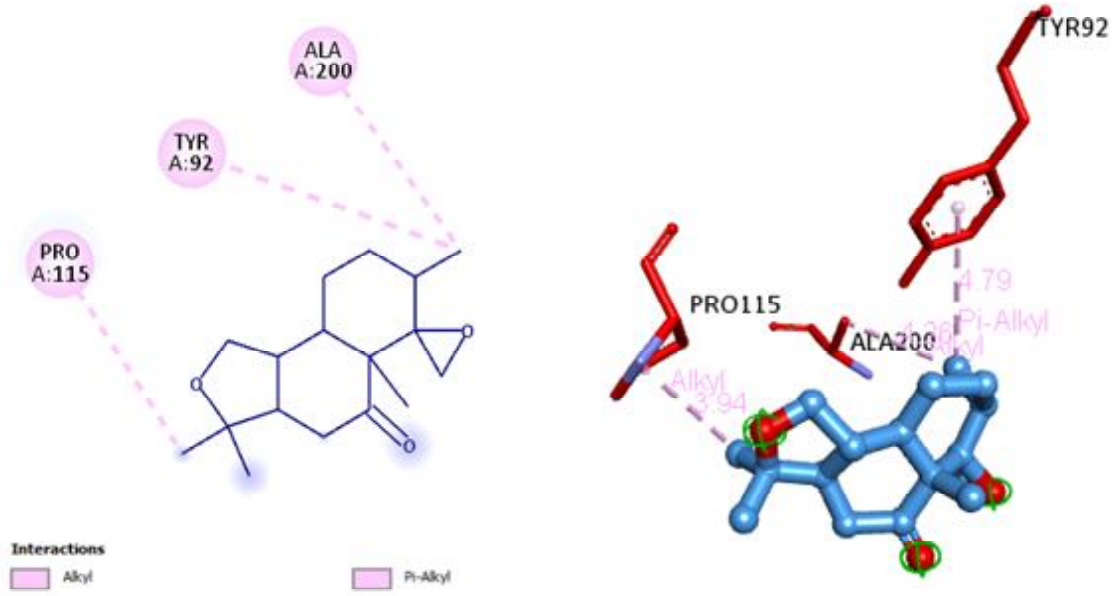

Figure 4. 2D and 3D molecular interactions of Limonoate against p53 protein

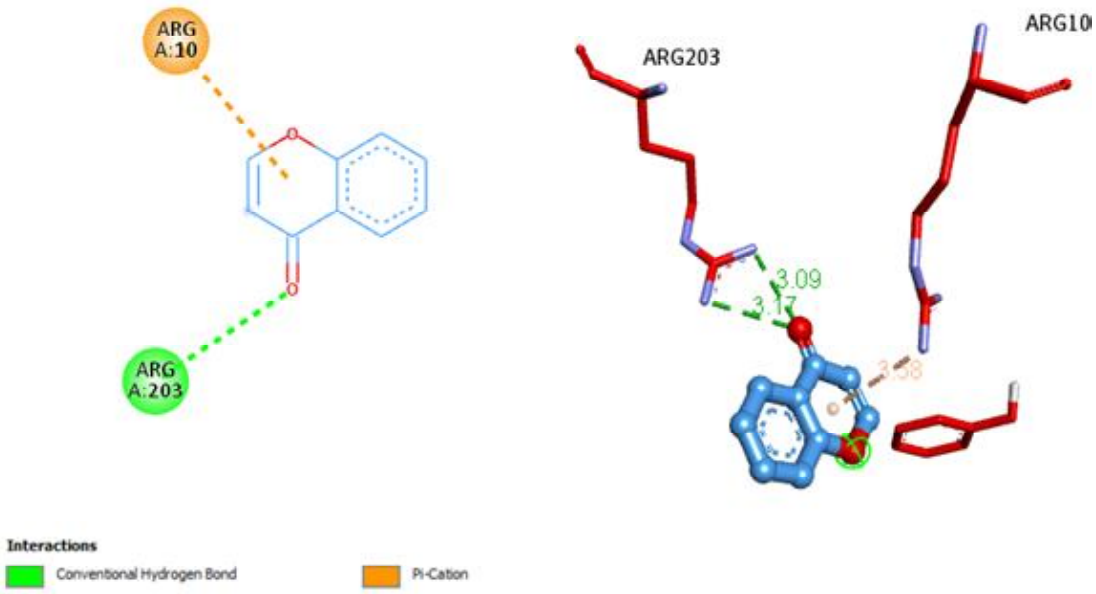

Figure 5. 2D and 3D molecular interactions of Luteolin against p53 protein

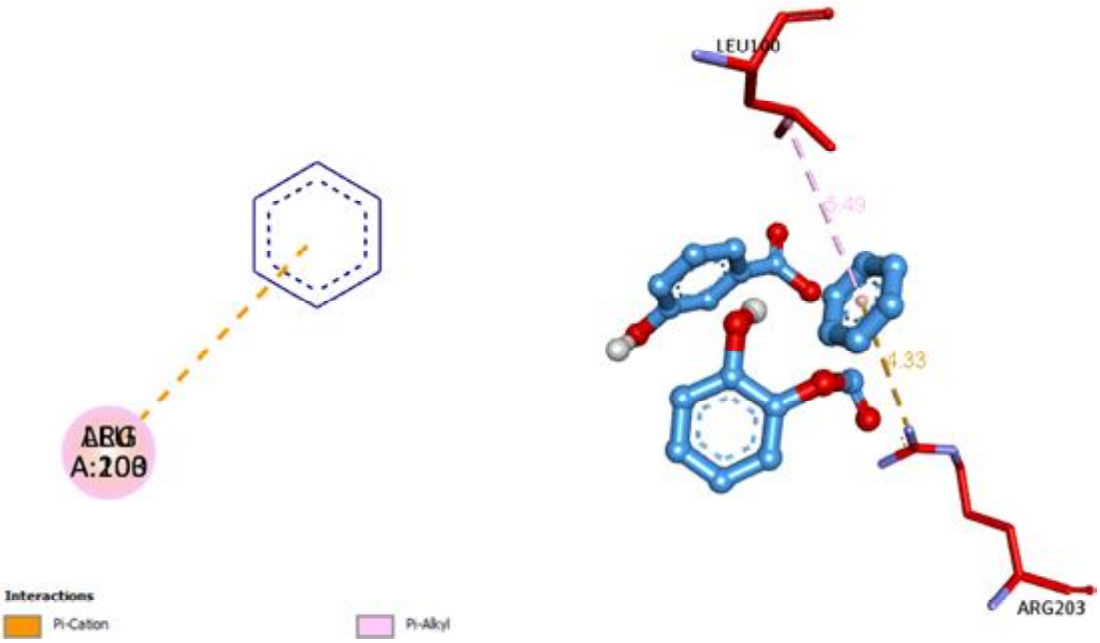

Figure 6. 2D and 3D molecular interactions of Myricetin 7-rhamnoside against p53 protein

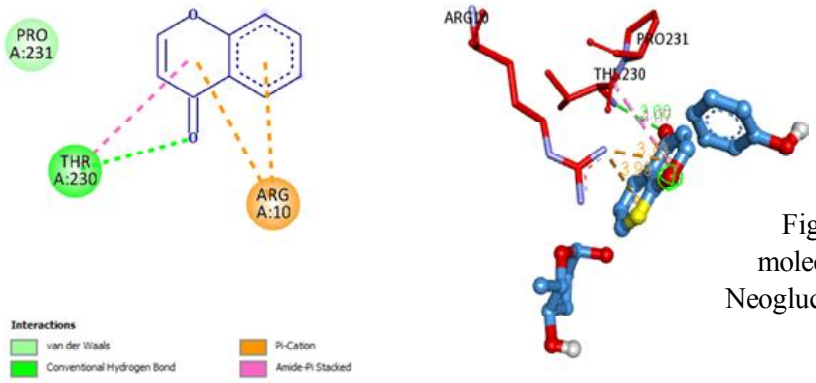

Figure 7. 2D and 3D molecular interactions of Neoglucobrassicin against p53 protein

Table-6a and 6b. Drug-likeness and Molecular Properties Properties of Selected Phytocompounds from *Hultholia mimosoides*

Sr no.	Compound name	Hydrogen bond donor	Hydrogen bond donor	Log p value	Molecular weight	No of violations
1	1-Hydroxytacrine	2	3	1.7831	214.267	0
2	Cavipetin D	2	5	7.3735	418.572	1
3	Convicine	7	11	-3.5858	305.242	2
4	Hibiscitrin	10	14	-1.0383	496.376	2
5	Limonoate	2	10	4.2726	504.53	1
6	Luteolin	4	6	1.99	286.238	0
7	Myricetin 7-rhamnoside	8	12	0.0819	464.378	2
8	Neoglucobrassicin	5	12	-0.4114	478.498	1
9	Retronecine	2	3	-0.4289	155.196	0
10	Sauroxine	1	3	2.2265	274.406	0

Table-6b

Sr no.	Compound name	Ligand efficiency (LE)	Lipophilic ligand efficiency (LLE)	Ligand-corrected lipophilic efficiency (LELP)
1	1-Hydroxytacrine	0.46619	3.654	3.8248
2	Cavipetin D	0.084042	-5.5357	87.735
3	Convicine	0.26494	7.6413	-13.535
4	Hibiscitrin	0.070867	2.8463	-14.651
5	Limonoate	0.060918	5.8712	-70.136
6	Luteolin	0.14877	0.28733	13.376
7	Myricetin 7-rhamnoside	0.046386	1.0339	1.7656
8	Neoglucobrassicin	0.08934	2.4302	-4.6049
9	Retronecine	0.62252	5.4204	-0.68897
10	Sauroxine	0.1552	0.036113	14.346

Table-7. ADMET Profile (Absorption, Distribution, Metabolism, Excretion, and Toxicity) of Selected Phytocompounds

Absorbtion	1	2	3	4	5	6	7	8	9	10
Water solubility	-3.104	-4.662	-2.389	-2.894	-2.683	0.096	-2.892	-2.739	-0.822	-3.163
Caco2 permeability	1.171	0.553	-0.557	-1.545	-0.291	81.13	-1.61	-0.693	1.435	1.539
Intestinal absorption	94.029	90.671	18.305	17.423	41.967	-2.735	38.019	5.936	99.202	92.195
Skin Permeability	-2.761	-2.735	-2.735	-2.735	-2.735	Yes	-2.735	-2.735	-2.739	-3.247
P-glycoprotein substrate	Yes	No	No	Yes	Yes	No	Yes	Yes	No	No
P-glycoprotein I inhibitor	No	No	No	No	No	No	No	No	No	No
P-glycoprotein II inhibitor	No	Yes	No	No	No	No	No	No	No	No
Distribution										
VDss	0.549	-0.952	0.823	1.288	-0.159	1.153	1.575	-0.754	0.311	0.856
Fraction unbound	0.33	0.054	0.802	0.282	0.584	0.168	0.167	0.471	0.507	0.556
BBB permeability	0.43	-0.558	-1.142	-2.474	-1.025	-0.907	-1.966	-1.658	0.474	0.349
CNS permeability	-1.99	-2.655	-3.989	-4.998	-3.338	-2.251	-4.319	-4.311	-2.974	-3.171
Metabolism										
CYP2D6 substrate	No	No	No	No	No	No	No	No	No	No
CYP3A4 substrate	No	Yes	No	No	Yes	No	No	No	No	No
CYP1A2 inhibitior	Yes	No	No	No	No	Yes	No	No	No	No
CYP2C19 inhibitior	No	No	No	No	No	No	No	No	No	No
CYP2C9 inhibitior	No	No	No	No	No	Yes	No	No	No	No
CYP2D6 inhibitior	No	No	No	No	No	No	No	No	No	No
CYP3A4 inhibitior	No	No	No	No	No	No	No	No	No	No
CYP2D6 substrate	No	No	No	No	No	No	No	No	No	No
Excretion										
Total Clearance	0.213	2.026	0.564	0.31	0.519	0.495	0.314	0.411	0.721	0.498
Renal OCT2 substrate	No	No	No	No	No	No	No	No	No	No
Toxicity										
Max. tolerated dose	0.119	-0.291	0.696	0.471	0.92	0.499	0.462	0.798	0.83	0.039
Oral Rat Acute Toxicity	2.588	1.901	2.528	2.515	2.397	2.455	2.553	2.631	2.482	2.559
Oral Rat Chronic Toxicity	1.333	0.403	3.346	3.914	1.642	2.409	3.389	3.905	5.559	0.683
Hepatotoxicity	Yes	No	Yes	No	Yes	No	No	Yes	No	No
Skin Sensitisation	No	No	No	No	No	No	No	No	No	No

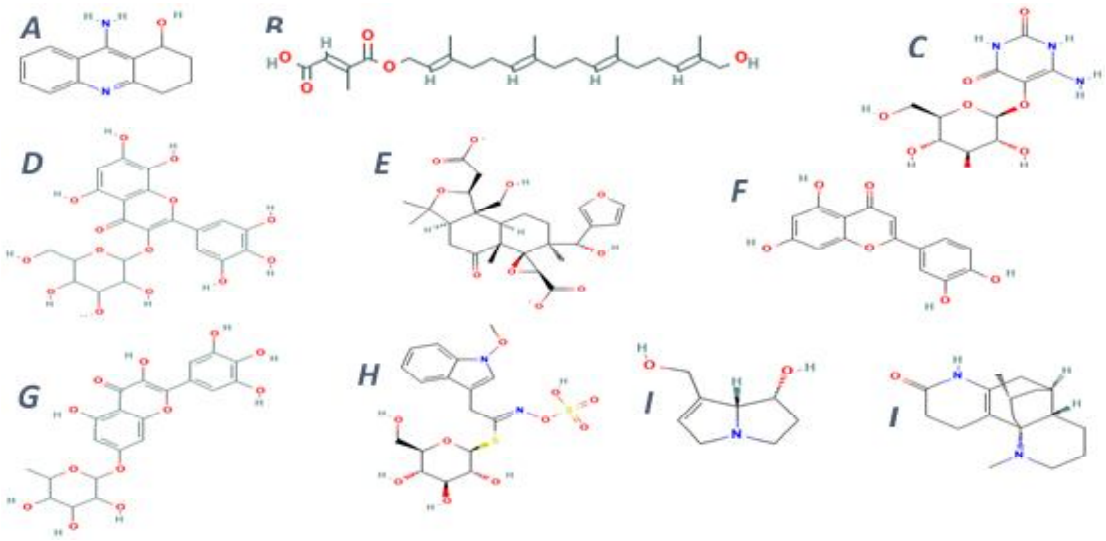

Figure 8. **A**-1-Hydroxytacrine**. B**- Cavipetin D**. C**- Convicine**. D**- Hibiscitrin. **E**- Limonoate**. F**-Luteolin**. G**-Myricetin 7-rhamnoside**.** **H**- Neoglucobrassicin**. I**- Retronecine**. J**- Sauroxine**.**

References :

1. Gaidhani, R. H., and G. Balasubramaniam, (2021). *Indian Journal of Medical Sciences*, *73*(1): 99–109. 10.25259/IJMS_92_2020
2. Green, D., and G. Kroemer, (2009). *Nature*, *458:* 1127–1130. https://doi.org/10.1038/nature07986
3. Han, M. Y., and E. H. Borazanci, (2023). *Frontiers in Oncology*, 13:1138759. https://doi.org/10.3389/fonc.2023.1138759
4. Liebermann, D. A., B. Hoffman, and D. Vesely, (2007). *Cell Cycle*, *6*(2): 166–170. https://doi.org/10.4161/cc.6.2.3789
5. Lipinski, C. A., (2004). *Drug Discovery Today: Technologies*, *1*(4): 337–341. https://doi.org/10.1016/j.ddtec.2004.11.007
6. Luo, W., J. Wang, H. Chen (2023). *Chinese Journal of Cancer Research*, *35*(5): 438. https://doi.org/10.21147/j.issn.1000-9604.2023.05.03
7. McCoy, J. G., C. A. Bingman, G. E. Wesenberg, and G. N. Phillips Jr, (2017). *Protein Data Bank*. Crystal structure of TP53-induced glycolysis and apoptosis regulator protein (PDB ID: 3DCY). http://doi.org/10.2210/pdb3DCY/pdb
8. Sander, T., J. Freyss, M. Von Korff, and C. Rufener, (2015). *Journal of Chemical Information and Modeling*, *55*(2): 460–473. https://doi.org/10.1021/ci500588j
9. World Cancer Research Fund, (n.d.). *Pancreatic Cancer Statistics*. Retrieved from https://www.wcrf.org/preventing-cancer/cancer-statistics/pancreatic-cancer-statistics